SUPPLEMENTARY MATERIAL

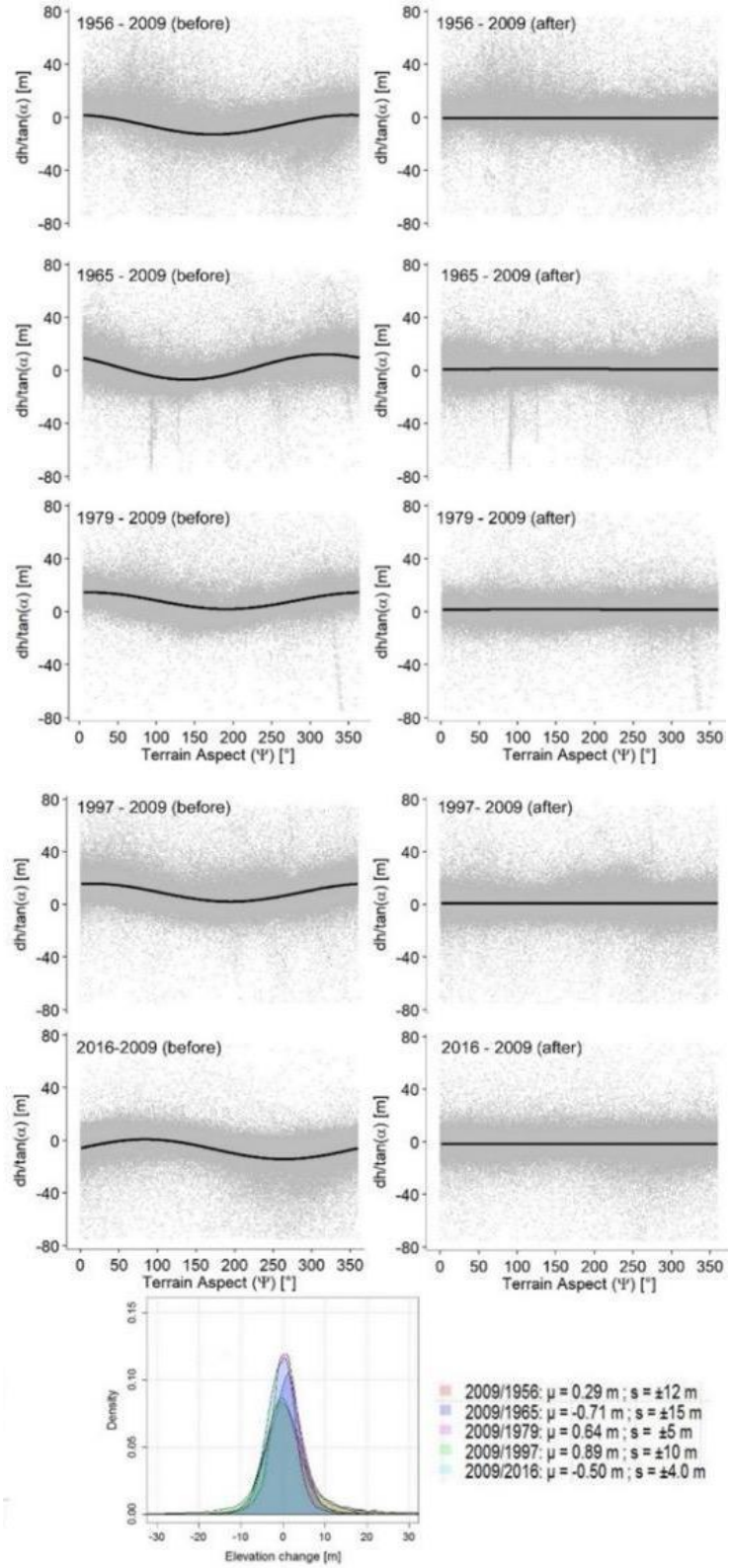

Fig S1. Comparison of the standardized elevation for each pixel (grey dots) by the tangent of the slope, as a function of the surface of the ground in the stable rocky areas in the vicinity of the ice cap, before and after co-registration, and the fitted cosine curve (black line). The resulting histograms of the residuals after adjustment for bias.

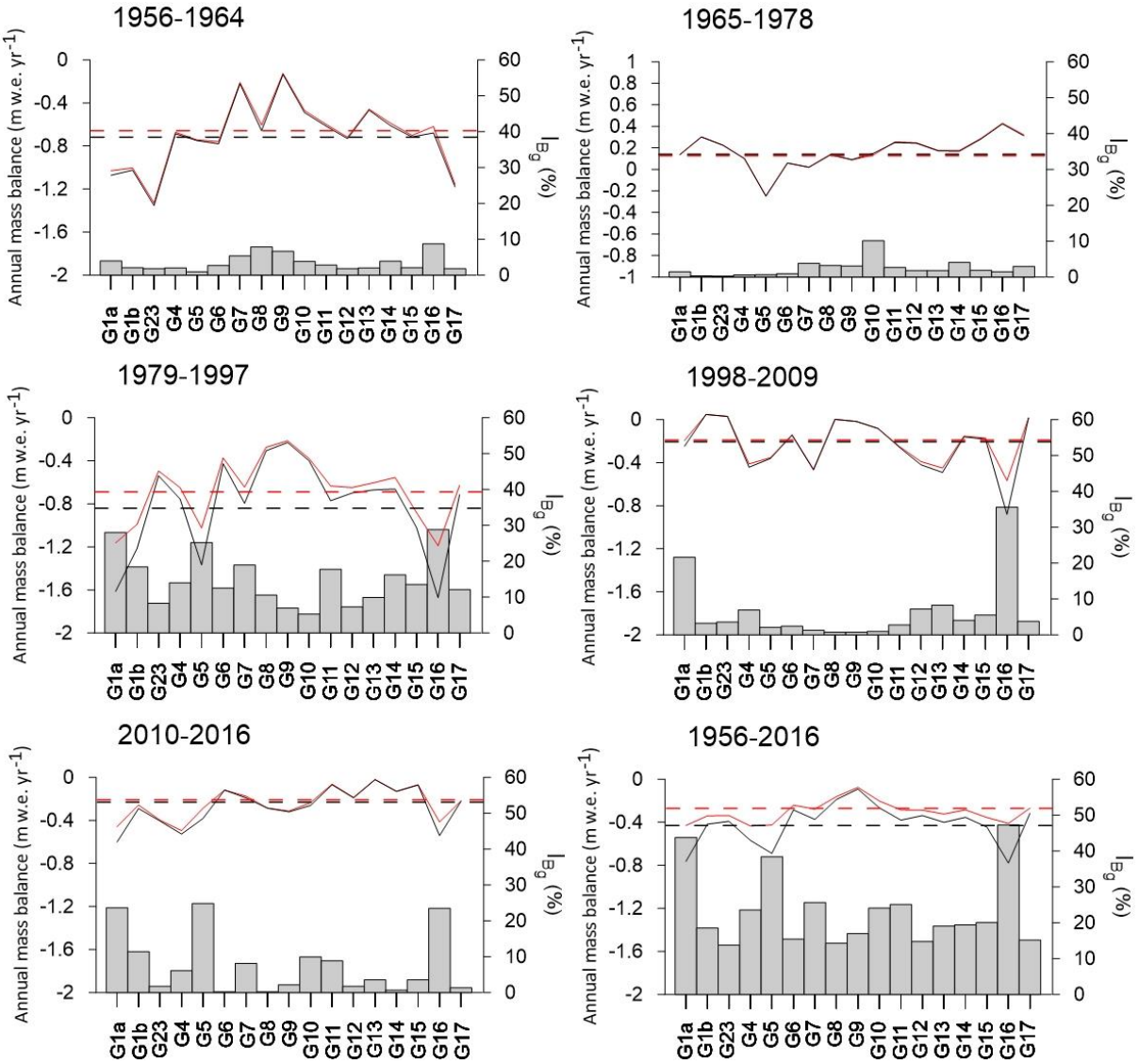

Fig S2. Annual glacier mass balance of 17 glaciers on the Antisana ice cap. Glacier-wide balance (solid black line), glacier-wide fixed balance (solid red line), and average annual mass balance (dashed line) for the sub-periods. The right vertical axes show the fraction of the balance on individual glaciers affected if the mean surface-area change is not taken into consideration.

Table S1. Characteristics of Antisana glaciers in the 1956-2016 period: Surface area in 2016 (S_{2016}), change in surface area (ΔS), maximum altitude (h_{max}), mean altitude (h_{mean}), median altitude (h_{medi}), minimum altitude (h_{min}), mean slope (α), azimuth ($\phi_{360°}$), orientation (ϕ_{sec}).

Name of the glacier	Code	S_{2016} [km^2]	$\Delta S_{1956/2016}$ [%]	h_{max} [m a.s.l]	$h_{mean1956/2016}$ [m a.s.l]	$h_{medi1956/2016}$ [m a.s.l]	$h_{min1956/2016}$ [m a.s.l]	α_{2016} [°]	$\phi_{360°}$	ϕ_{sec}
(α)	G1a	0.17±0,03	88	5218	4773 / 4982	4758 / 4982	4435 / 4800	28	14	NE
(β)	G1b	0.71±0,03	57	5611	4887 / 5034	4848 / 4962	4325 / 4550	32	52	NE
-	G2,3	3.17±0,03	28	5678	4908 / 5039	4871 / 5033	4067 / 4367	29	54	NE
-	G4	1.22±0,02	47	5582	4742 / 4772	4699 / 4723	4342 / 4434	27	75	E
-	G5	0.26±0,02	77	5070	4688 / 4791	4676 / 4792	4398 / 4671	31	130	SE
Azufral	G6	1.14±0,02	31	5605	4870 / 4838	4875 / 4761	4197 / 4462	32	148	SE
-	G7	0.20±0,01	51	5238	4800 / 4900	4804 / 4899	4480 / 4640	37	169	S
De la Caldera	G8	1.88±0,03	29	5640	4990 / 5090	4997 / 5060	4295 / 4606	32	181	S
Cimarrones Oriental	G9	0.14±0,01	31	5420	5034 / 5076	5025 / 5079	4714 / 4801	39	190	S
Cimarrones Central	G10	0.18±0,01	21	5522	5004 / 5046	4934 / 4983	4649 / 4668	40	219	SO
Cimarrones Occidental	G11	0.23±0,01	47	5538	5008 / 5077	4911 / 4964	4682 / 4668	37	249	SO
Great West Los Crespos	G12	1.56±0,03	30	5698	5067 / 5149	5008 / 5121	4658 / 4718	28	254	SO
Los Crespos	G13	0.98±0,02	38	5703	5091 / 5204	5017 / 5157	4778 / 4845	29	266	O
Guagraialina or Los Crespos Norte	G14	0.32±0,01	39	5469	5013 / 5093	4979 / 5064	4704 / 4830	28	291	O
(α, β)	G15	0.53±0,01	40	5688	5106 / 5226	5048 / 5211	4776 / 4855	31	313	NO
-	G16	0.03±0,01	95	5299	4931 / 5121	4906 / 5127	4750 / 4965	32	330	NO
-	G17	1.16±0,02	30	5697	5067 / 5210	5007 / 5267	4467 / 4645	26	356	N

Appendix S1. Seasonal climate conditions during key periods

Figure S3 shows no clear relationship between temperature and precipitation anomalies whatever the sub-period considered, but particular features can nevertheless be underlined. We can confirm that cold conditions prevailed until the late 1970s. Warm periods appear to have been enhanced after the beginning of 1980s and have lasted longer in the last decade. Regarding precipitation, the most marked temporal variability occurred in the 1965-1978 and 1979-1997 periods, in which extremely positive or negative mass balances were observed, variability then decreased markedly in the two last decades. It is worth recalling that decadal mass balance variability matches the positive and negative anomalies observed in the Pacific Ocean.

Finally, we stress that in the two key quarters (MAM and SON), 27% of the years can be considered as anomalous, but the quarters differed from one year to the other. Conditions were very cold during the MAM quarter in 10 of the years, and 70% of the cold periods were characterised by humid conditions. During the SON quarter, conditions were more scattered with very cold conditions in 11 of the years during the 1950-1980 period, and with humid conditions in 55% of the years. In the MAM quarter, the strongest "El Niño" events occurred in 1998 (2015/2016) in a wet (dry) context, respectively, while the "La Niña" event of 1999/2000 changed from very wet-cold to dry-cold conditions.

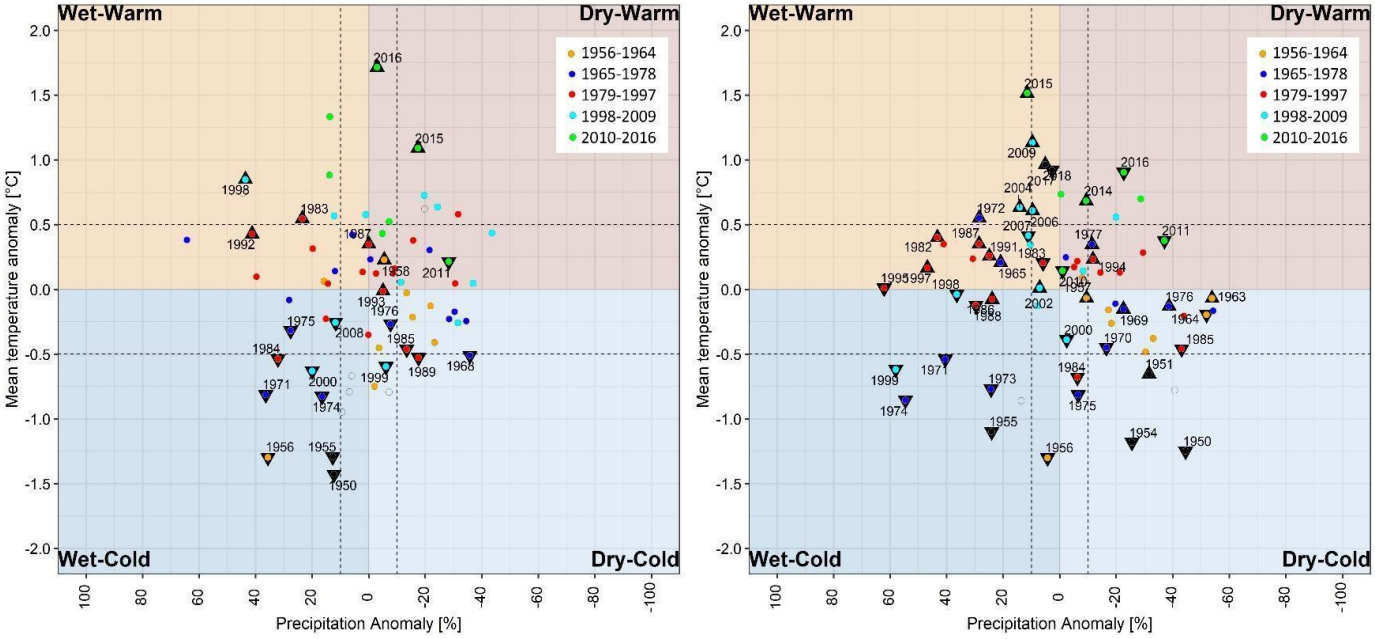

Fig S3. Scatterplot of MAM (right) and SON (left) showing temperature and precipitation anomalies in ERA data for the period 1950-2018. The dashed lines show climatic threshold values. Coloured dots represent the centred mass balance for the five sub-periods and the empty circles indicate years with no mass balance. Positive/negative years observed in the Pacific Ocean are indicated by upright/inverted triangles.

Two contrasting situations can thus be highlighted. On the one hand, in a wet-cold context during the MAM quarter, solid precipitation is expected to cover the surface of the glaciers and to remain in place until the following SON quarter, combined with continuous cloudiness, which can reduce the effects of incoming solar radiation, thereby weakening ablation. This situation may be accentuated during the cold "La Niña" events. On the other hand, if precipitation is scarce and/or liquid during warm periods, combined with less cloud cover, incoming solar radiation will enhance ablation by increasing ice melt during the equinoxes. In fact, at the scale of the Antisana ice cap, the glaciers' response is in good agreement with the cold/warm periods illustrated by the Southern Oscillation Index (SOI). At a sub-decadal time step, *in-situ* observations revealed a strong influence of ENSO episodes on glacier response, in this context, it is reasonable to assume a cumulative effect of ENSO events at multi-decadal scale.